

Space Charge Measurement Using a Small Sphere as a Probe

By

Osamu YAMAMOTO*, Toshihiko KOUNO*,
Chikasa UENOSONO* and Muneaki HAYASHI*

(Received June 30, 1982)

Abstract

A method for measuring the space charge produced by impulse corona in an air gap has been developed, using a small sphere as a probe. The probe is located far from the corona volume, and is connected to earth through resistance or capacitance. The probe induces a current or charge by electrostatic induction from the space charge.

Since the induced charge on the probe is proportional to the space charge, it is possible to analyze the magnitude and polarity of the space charge from the probe signal.

It is also possible to analyze the temporal variation caused by corona growth or movement of the space charge.

1. Introduction

The discharge in air at long gap by applying high voltage develops from corona via leader stroke to arc discharge.

It has been said that the development is affected by the space charge produced in the gap by the corona. Many studies have been performed to clarify the temporal and spatial behavior of the space charge.¹⁾⁻⁵⁾

This paper describes the method of space charge measurement and its application in the long gap and non-uniform electric field in air, using a small metal sphere as a probe. This probe has a radius of 0.5 cm, and is located at a distance of 1.5 times the gap length or more from the gap axis. Thus, it can only detect the current or charge caused by electrostatic induction from the space charge, without including any true charge from the discharge.

A coefficient of proportionality between the induced charge and the space charge is needed for evaluating the magnitude of the space charge produced by corona from the data obtained by the probe. This coefficient can be obtained by experiment or by calculation based on Green's Reciprocal Law. The polarity of the space charge can be analyzed exactly from the induced current on the probe.

* Department of Electrical Engineering

By analyzing the probe signal, it is possible to discriminate between the corona discharge and the glow discharge. The probe affects the applied field. However, this effect is negligible, as calculated by the Surface Charge Method.

2. Principle of space charge measurement

2.1 General comment

As shown in Fig. 1, probes were located at a distance of 1.5 times or more the gap length, measured from the axis of the rod-plane air gap. Then, each probe received an induced charge by electrostatic induction from the space charge produced by the corona discharge. To measure the induced charge, two circuits, presented in Fig. 2, were used. Fig. 2 (a) is a differential circuit⁶⁾ and Fig. 2 (b) is an integral circuit.⁷⁾ The former is used to measure the variation of the induced charge as the current flows through resistance R to earth. The latter is used to measure the induced charge directly by using the capacitance C which is connected between the probe and earth.

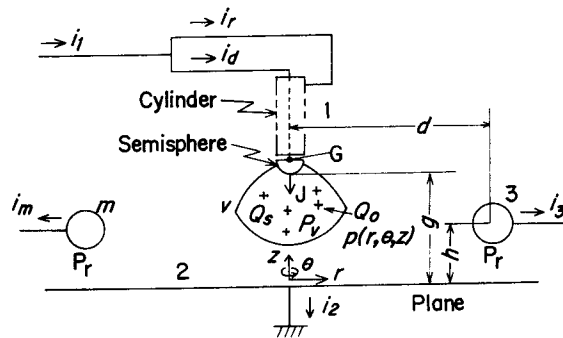


Fig. 1. Arrangement of probes and their currents.
(P_r ; probe, $d=1.5g\sim 2.0g$)

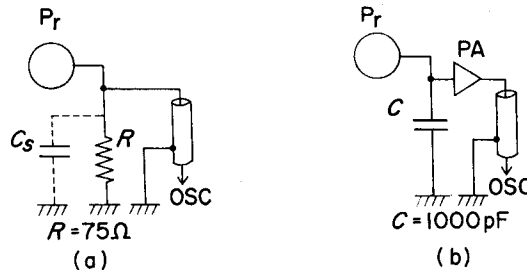


Fig. 2. Circuits for space charge measurement.
(a) Differential circuit
(b) Integral circuit

2.2 Principle

During the corona growth, the space charge is produced in a corona volume v , as shown in Fig. 1. By ionization, electrons, positive and negative ions are generated in this volume. They all move under the influence of the electric field. However, the electrons move faster than the ions. So, the residual electrons and ions remaining in the volume constitute the space charge. The density and magnitude of the space charge are denoted by ρ_v and Q_s , respectively.

At first, the induced charge on the probe due to the point charge (Q_0) was analyzed. In this analysis, the plane electrode was assumed to be infinitely large.

The relationship of the potential V_n and charge Q_n ($n=1, 2, \dots$) of these conductors is given by Eq. 1, where suffixes $n=1, n=2$ are given to the rod and plane electrodes respectively, and $n \geq 3$ to the probes.

$$\begin{pmatrix} P_{11} & \dots & P_{1n} \\ \vdots & & \vdots \\ P_{n1} & \dots & P_{nn} \end{pmatrix} \begin{pmatrix} Q_1 \\ \vdots \\ Q_n \end{pmatrix} + Q_0 \begin{pmatrix} P_{10} \\ \vdots \\ P_{n0} \end{pmatrix} = \begin{pmatrix} V_1 \\ \vdots \\ V_n \end{pmatrix} \quad \dots\dots(1)$$

In Eq. 1, P_{mn} is the potential coefficient between the conductors m and n , and P_{m0} ($m=1, 2, \dots$) is the potential coefficient between Q_0 and the conductor m .

From Eq. 1, the charges on the conductors are given by:⁸⁾

$$\begin{pmatrix} Q_1 \\ \vdots \\ Q_n \end{pmatrix} = \begin{pmatrix} K_{11} & \dots & K_{1n} \\ \vdots & & \vdots \\ K_{n1} & \dots & K_{nn} \end{pmatrix} \begin{bmatrix} (V_1 - P_{10}Q_0) \\ \vdots \\ (V_n - P_{n0}Q_0) \end{bmatrix}, \quad \dots\dots(2)$$

where K_{mn} is the induction coefficient between the conductors m and n . Since the potentials V_2 and V_n ($n \geq 3$) were found experimentally to be negligible compared to the potential of the rod (V_1), which was the applied voltage to the rod, they were thus taken as zero. Then, Q_m is simply given by:

$$Q_m = K_{m1}V_1 - Q_0 \sum_{i=1}^n K_{mi}P_{i0} \equiv K_{m1}V_1 + Q_0D_m, \quad \dots\dots(3)$$

provided that $-\sum_{i=1}^n K_{mi}P_{i0} = D_m$.

In Eq. 3, $K_{m1}V_1$ is the induced charge on the conductor m caused by applying voltage to the rod. From now on, we shall call D_m ($m \geq 3$) the induction coefficient of the probe. D_m depends on the position of the probe and Q_0 . The determination of D_m is described in Section 2. 4.

In the differential circuit, the current I_m flowing from the probe to earth is given by differentiating Q_m with respect to time as given by:

$$I_m = -K_{m1} \frac{dV_1}{dt} - \frac{\partial Q_0 D_m}{\partial t} \equiv i_{Vm} + i_m, \quad \dots\dots(4)$$

provided that $-K_{m1} \frac{dV_1}{dt} = i_{V_m}$ and $-\frac{\partial Q_0 D_m}{\partial t} = i_m$.

The component i_{V_m} is the displacement current due to applying voltage to the rod. i_m is the displacement current due to the movement of Q_0 , or a change in its quantity.

Thus, assuming Q_0 to be constant, we can analyze its movement from the change in i_m .

The charge q_m which was induced on the probe by the space charge in the corona volume, excluding $K_{m1}V_1$, is given by:

$$q_m = \int_v D_m \rho_v dv \quad (m \geq 3), \quad \dots\dots(5)$$

where ρ_v depends on the time and position in the gap, and v depends on the time. By differentiating q_m , the current of the probe is given by Eq. 6.

$$i_m = -\frac{\partial}{\partial t} \left(\int_v D_m \rho_v dv \right) \quad \dots\dots(6)$$

Thus, from the above Eq., the differential circuit detects the temporal variation of the space charge. This current (i_m) is detected by measuring the potential drop across the resistance R , as shown in Fig. 2 (a). On the other hand, the induced charge (q_m) on the probe is detected by measuring the potential drop across the capacitance ($= -q_m/C$), as shown in Fig. 2 (b).

As mentioned later, the time constant of the differential circuit is very short (less than 1 ns). Hence, this is useful for measuring high speed variations of the space charge. However, the time constant of the integral circuit is about 30 ms, and is thus useful for measuring slow variations of the space charge.

2.3 Electric field distortion by a probe

The introduction of the probe in the air gap distorts the electrostatic field. Should the electric field on the surface of the probe become high enough as to cause a secondary discharge from the surface, then a true space charge measurement in the air gap is impossible. This section describes the distortion of the electric field and the field strength of the probe surface, calculated by the Surface Charge Method.⁹⁾

All numerical quantities used in this calculation are taken from the actual experimental set-up. That is, a probe is located at a distance d from the gap axis and at a height h above the plane electrode (See Fig. 1.) The rod electrode radius (r_r) is equal to the probe radius ($r_{pr}=0.5$ cm). In this paper, the probe location for $d=1.5g$ and $h=0.5g$ is called "Standard Position", where g is the

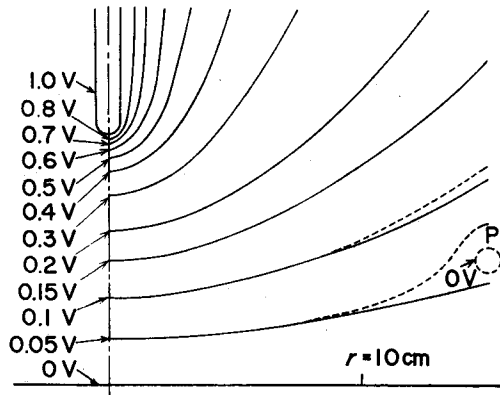


Fig. 3. Variation of potential distribution caused by the probe. (— without probe. ---- with probe. $g=10$ cm, $r_r=r_{pr}=0.5$ cm, $d=15$ cm, $h=5$ cm)

gap length of the rod-plane gap.

Fig. 3 shows the equipotential lines for a 10 cm gap with and without the probe. From the Fig., it is found that only the electric field near the probe is distorted, or else the entire field is generally undistorted by the probe. For example, at a point where $r=10$ cm and $z=5$ cm (See Fig. 1.), the electric field strength is found to be 5% stronger with the probe than without the probe. Since the actual corona does not spread out to this point, the distortion of the electric field due to the probe can thus be neglected.

The maximum electric field strength E_{m1} at the top of the rod without the probe was calculated to be $1.5 \times V_1$ (V/cm). The value of E_{m1} was found to be almost constant for the probe located at $d > 1.5g$. At the Standard Position, the maximum electric field strength E_{m3} , on the surface of the probe was calculated to be $0.15 \times V_1$ (kV/cm). When the probe location is varied, E_{m3} varies considerably whereas E_{m1} is constant.

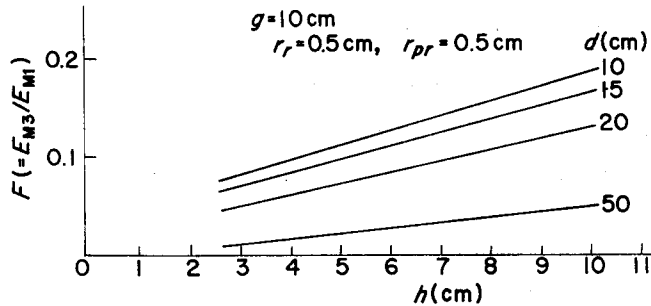


Fig. 4. Variation of the ratio (F) with the location of the probe.

Fig. 4 shows the relationship between h and the ratio $F (=E_{m3}/E_{m1})$ with d as the parameter. From this Fig. F increases with an increase in h . Since E_{m1} is constant, it follows that E_{m3} decreases with a decrease in h , and increases with a decrease in d .

Now, from the experiment, the 50% flashover voltage (V_{50}) of a 10 cm gap was about 80 kV. So that E_{m3} for the Standard Position is 12 kV/cm ($=0.15 \times 80$ kV/cm). In an atmosphere without humidity, it needs at least 25 kV/cm to ionize the air molecules by electron collision.¹⁰⁾ E_{m3} is so low compared with the required value for ionization that no discharge occurs from the surface of the probe. However, if the applied voltage is equal to or higher than V_{50} , a corona discharge is observed from the probe. This discharge is considered to be caused by the effect of the space charge produced by the corona discharge from the rod electrode. Therefore, with applied voltage higher than or equal to V_{50} , it is necessary to decrease h or increase d from the Standard Position for decreasing the electric field strength of the probe surface.

2.4 Induction coefficient D_m

In this section, using Green's Reciprocal Law, the coefficient D_m for a probe against Q_0 is derived. In order to use this law, the following two conditions are necessary: (a) Excluding the point charge in the gap, the potential of conductor m , and all other conductors are V_m and zero respectively. It is also supposed that the potential of the optional point p in the air gap is V_p . (b) Locating Q_0 at the point p , the potential of all the conductors is supposed to be zero. Hence the charge $Q_m^{(1)}$ induced on the probe m , under the condition (b), is given by Eq. 7, in accordance with Green's Reciprocal Law.¹¹⁾

$$Q_m^{(1)}/Q_0 = -V_p/V_m \quad \dots\dots(7)$$

$Q_m^{(1)}$ is also derived by putting $V_1=0$ in Eq. 3, which yields $Q_m^{(1)}=Q_0 \times D_m$. From these Eqs., we get D_m as follows.

$$D_m = -V_p/V_m \quad \dots\dots(8)$$

In this paper, D_m is calculated using the Surface Charge Method. Fig. 5 (a) and (b) shows the D_m for a probe ($m=3$), with h and d as parameters respectively.

In these Figures, Q_0 was assumed to exist on the gap axis (z axis) (See Fig. 1.) From these Figures, it is seen that D_m is zero when Q_0 exists on the surface of each electrode and becomes maximum when it exists at a distance of 2~3 cm from the surface of the rod electrode.

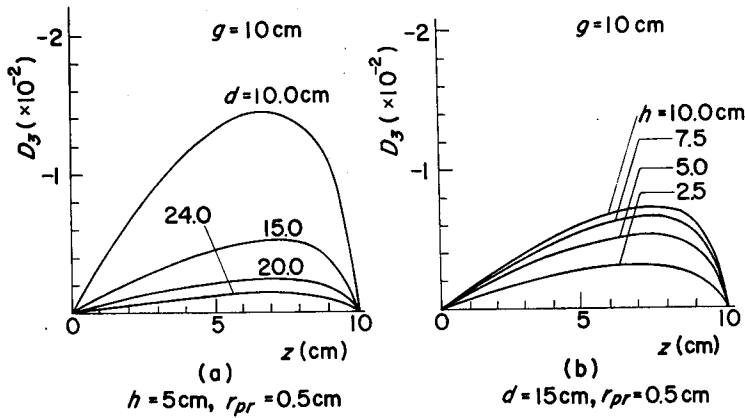


Fig. 5. Calculated coefficient D_3 from a point charge on the gap axis to the probe.

2.5 Consideration for space charge measurement

The current flowing through the rod into the air gap (i_1), and flowing through the plane to earth (i_2), and the currents of probes ($i_m, m \geq 3$) are governed by the following relation.

$$i_1 = i_2 + i_3 + \dots + i_n \quad \dots\dots(9)$$

Assuming that the corona starts from the surface of the semisphere at the tip of the rod, and that the corona volume is v at $t=t_0+\tau$, then the amount of the space charge Q_s during the corona growth is given by integrating ρ_v in the volume. On the other hand, Q_s is injected into the gap through the semisphere. Q_s is given by integrating this injection current during the corona growth. This current is denoted by J in Fig. 1. Hence, we have following relationships between Q_s, ρ_v , and J .

$$Q_s = \int_v \rho_v dv = \int_{t_0}^{t_0+\tau} J dt \quad \dots\dots(10)$$

Now, Q_s yields charge q_1 on the rod, and q_2 on the plane by electrostatic induction. These charges can be represented by Eq. 5, where D_1 and D_2 are the induction coefficients of the rod and plane respectively. Thus, assuming that all the electric flux from Q_s links with every conductor, the relationship between Q_s and $q_m (m=1,2,\dots,n)$ is represented by Eq. 11.

$$Q_s = \left| \sum_{m=1}^n q_m \right| = \left| \sum_{m=1}^n \int_v D_m \rho_v dv \right| \quad \dots\dots(11)$$

Therefore each electrode has a current due to change in ρ_v during the corona

growth. These currents are given by the following Eqs.

(i) In the rod:
$$-\frac{\partial q_1}{\partial t} = -\frac{\partial}{\partial t} \left(\int_v D_1 \rho_v dv \right)$$

(ii) In the plane:
$$-\frac{\partial q_2}{\partial t} = -\frac{\partial}{\partial t} \left(\int_v D_2 \rho_v dv \right)$$

In this consideration, it is necessary to take into account the current accompanying the glow or arc discharge. This current is denoted by J_{con} and is called the conduction current to distinguish it from the current J . Hence, the total current in the rod (i_1) caused by discharge is given by adding these currents:

$$i_1 = (J + J_{con}) + \frac{\partial q_1}{\partial t} \equiv i_d + i_r, \quad \dots\dots(12)$$

provided that $i_d = J + J_{con}$ and $i_r = \partial q_1 / \partial t$. Since q_1 is mainly induced on the cylindrical part of the rod electrode, i_r flows from here to the high potential line. (See Fig. 1.)

Similarly, the total current flowing through the plane (i_2) to earth is given by Eq. 13.

$$i_2 = J_{con} - \partial q_2 / \partial t \quad \dots\dots(13)$$

However, since the probes are located far from the corona volume, the currents flowing through them to earth do not include the conduction current, as shown by Eq. 6.

From these currents, the total charge Q_d , which is injected from the semisphere into the air gap in accordance with the growth of the corona and glow discharge, is given by integrating i_d , as represented in Eq. 14.

$$Q_d = \int_{t_0}^{t_0+\tau} (J + J_{con}) dt = \int_{t_0}^{t_0+\tau} i_d dt \quad \dots\dots(14)$$

During this discharge, the charge which flows from the plane to earth ($Q_d^{(1)}$) and the induced charge on the probe rae given by Eq. 15 and Eq. 16 respectively.

$$Q_d^{(1)} = \int_{t_0}^{t_0+\tau} i_2 dt \quad \dots\dots(15)$$

$$q_m = -\int i_m dt \quad (m \geq 3) \quad \dots\dots(16)$$

For a discharge that does not maintain glow and arc discharges, the current is considered to be zero so far as J_{con} is concerned. In this case, Eq. 14 is same as Eq. 10, giving the next relationship.

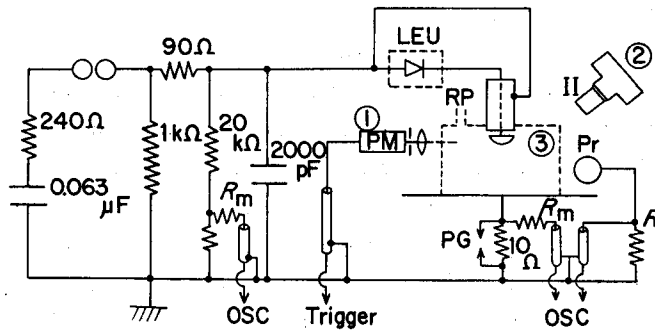
$$Q_d = Q_s \dots\dots(17)$$

3. Space charge measurement using the probe

The space charge in the air gap produced by the corona discharge by applying the lightning impulse voltage is measured by a probe. The currents in the rod and plane electrodes are also measured simultaneously.

3.1 Experimental procedure

The circuit layout of the apparatus used in this experiment is shown in Fig. 6. An impulse wave form of $\pm(1.8 \times 50) \mu s$ was produced by an impulse voltage generator. The radius of the rod and plane electrodes was 0.5 cm and 50 cm respectively. Both electrodes were made of brass. To measure the current i_d of the rod electrode, the rod tip semisphere and the remaining cylindrical parts were isolated, as shown in Fig. 1.



- PG ; Protection gap, RP ; Rotary pump,
- II ; Image intensifier, R_m ; (For impedance matching)
- ① ; Photomultiplier, ② ; Still camera with II,
- ③ ; Vaccum chamber.

Fig. 6. Experimental apparatus.

In this experiment, two methods of gap arrangement were employed. (i) The impulse voltage was applied to the rod with the plane electrode earthed. (ii) The impulse voltage was applied to the plane with the rod electrode earthed. The former method is called the normal arrangement, while the latter is called the reverse arrangement. As mentioned earlier, the radius of the probe is 0.5 cm. The time constant of the differnetial circuit (See Fig. 2 (a)) is given by $R \times C_s$, where C_s is the stray capacitance of the probe, and is assumed to be less than 1 pF. R was chosen to have the same value as the characteristic impedance (75Ω) of the transmission cable. Thus, for this case, the time constant of the differntial

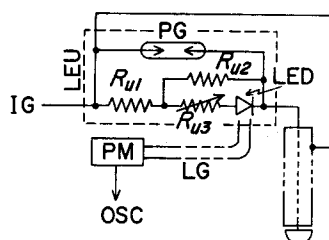
circuit is less than 1 ns. For the integral circuit (See Fig. 2 (b)), the voltage across the capacitance C ($=1000$ pF) is connected to the oscilloscope through the pre-amplifier (PA). PA is used for impedance matching and has an input impedance of $30\text{ M}\Omega$ and an output impedance of 75Ω . The time constant of the integral circuit is given by $R_{in} \times C$, where R_{in} indicates the input impedance of PA, and is found to be about 30 ms.

As shown in Fig. 6, to detect the light emitted by the corona, a photo-multiplier, a quartz lens and a slit were arranged near the air gap. To observe the currents and space charge, using the oscilloscope, a light pulse from the photo-multiplier was supplied to the external trigger pulse generator of the oscilloscope. By using this trigger system, the oscilloscope sweep starts just before the currents and space charge signals arrive at the scilloscope. This is because the length of the light pulse cable is shorter than those of the currents and the space charge. A still camera with an image intensifier was also used to observe the weak image of the corona discharge. As mentioned later, the space charge was also measured for the case of a glow discharge in a low pressure air gap. It was only for this case that a vacuum chamber, made of acilile ($30 \times 30 \times 20\text{ cm}^3$), was used.

In both gap arrangements, the earthed electrode was earthed through a resistance of 10Ω . Thus, the rod current i_1 for the reverse arrangement, and the plane current i_2 for the normal arrangement, were detected using this resistance.

For the normal arrangement, the current i_d of the rod electrode was measured using a light emitting unit (LEU), as shown in Fig. 7.¹²⁾ The response of the LEU against the stepwave was experimentally found to be 50 ns.

To observe the above mentioned currents and space charge, two double beam



$$R_{U1} = 25\ \Omega, \quad R_{U2} = 100\ \Omega, \quad R_{U3} = 10 \sim 100\ \Omega,$$

LEU; Light emission unit, PG; Protection gap, LED; Light emission diode (Monsant MV5020), LG; Light guide (20m), PM; Photo-multiplier (Toshiba PM 55).

Fig. 7. Circuit for measuring the current of the rod electrode.

oscilloscopes (Tek type 556 and 7844) were used. The rise time of the vertical amplifier for type 556 and 7844 is designated to be 7 ns and 1.9 ns respectively.

3.2 Space charge measurement in rod-plane air gap

This section describes the relationship between the magnitude of the space charge produced by the corona discharge, and the induced charge on the probe. With the probe fixed at the Standard Position, the gap length varied from 7.5 to 20 cm. The experiment was performed under ordinary atmospheric pressure. The applied voltage (V_1) varied from the corona onset voltage (V_{on}) up to a certain voltage (V_{bs}). This was the minimum voltage that just caused the corona to bridge over the gap. The relationships of V_{on} and V_{bs} against the gap length are shown in Fig. 8.

Fig. 9 shows oscillographs of the probe current i_3 of the differential circuit, the induced charge q_3 of the integral circuit and the current i_d of the rod electrode.

The relation between Q_d and q_3 , are presented in Fig. 10, with g as the para-

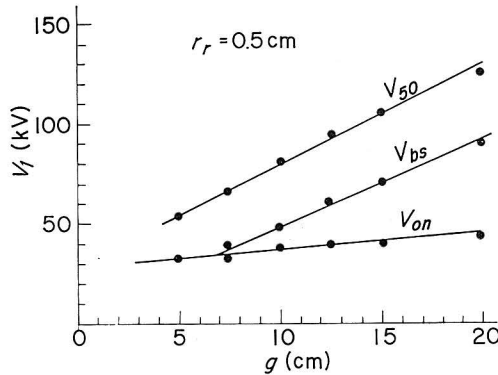


Fig. 8. Characteristics of V_{on} , V_{bs} and V_{50} vs. gap length (g).

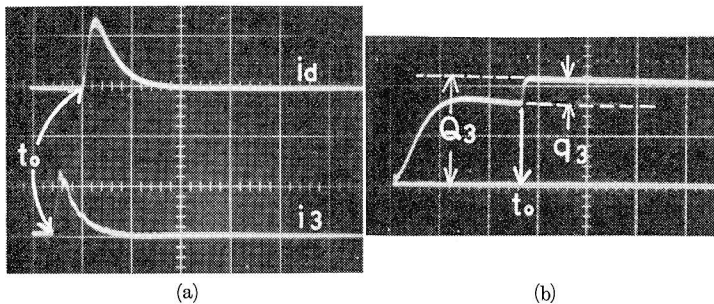


Fig. 9. Oscillographs of i_d , i_3 and q_3 . (normal arrangement, $V_1 = +44$ kV, $g = 10$ cm, $d = 15$ cm, $h = 5$ cm)

- (a) i_d ; 0.77 A/div., i_3 ; 5.3 mA div. ($0.2 \mu s$ /div.)
- (b) q_3 ; -1.7×10^{-8} C/div. ($0.2 \mu s$ /div.)

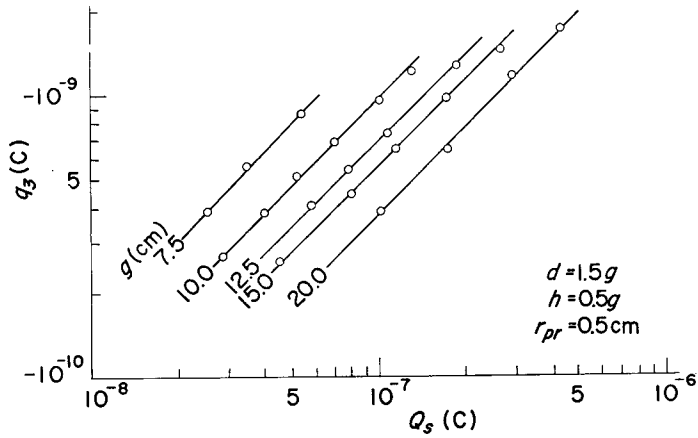


Fig. 10. Relations between Q_d and q_3 with g as the parameter.

meter.

Under the condition that $V_{on} < V_1 < V_{bs}$, the corona does not bridge over the gap, and therefore, J_{con} need not be taken into account in Eq. 14. Consequently, we get $Q_d = Q_s$, as shown in Eq. 17. Thus, the relation between Q_s and q_3 can be obtained from Fig. 10, and it is found that q_3 increases proportionally in accordance with an increase of Q_s . From these results, the relationship between Q_s and q_3 can be represented as follows:

$$Q_s = Aq_3, \tag{18}$$

where A is a proportionality ratio for each gap length. A increases linearly with the gap length as shown in Fig. 11.

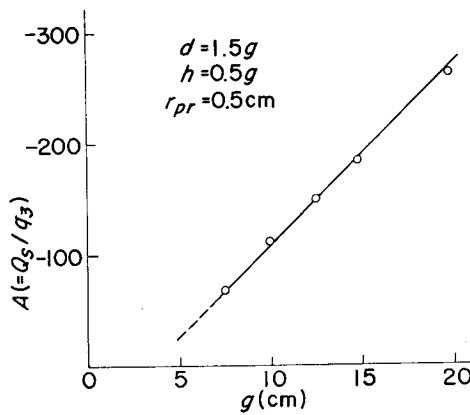


Fig. 11. The ratio A vs. g for the probe located at the Standard Position.

To estimate the magnitude of the space charge from the data obtained by the probe, it is necessary to assume that the space charge distribution is known. However, if A is already known, then Q_s can be estimated by Eq. 18.

The proportionality ratio for the probe not located at the Standard Position is determined as follows. At first, let the induced charge on the probe be $q_3(d)$, and the proportionality ratio be $A(d)$ for the probe location $d(\neq 1.5 g)$ with $h=0.5 g$. Then, Q_s is given by

$$Q_s = A(d) \cdot q_3(d) . \quad \dots\dots(19)$$

From Eqs. 18 and 19, the following relation is obtained.

$$q_3(d)/q_3 = A/A(d) \equiv B(d) \quad \dots\dots(20)$$

By using the above Eq., we get

$$Q_s = [A/B(d)] \cdot q_3(d) \quad \dots\dots(21)$$

For the probe location $h(\neq 0.5 g)$ with $d=1.5 g$, by the same procedure as mentioned above, Q_s is given by Eq. 22 below provided that $q_3(h)/q_3 \equiv B(h)$, where $q_3(h)$ is the induced charge on the probe located at h with $d=1.5 g$.

$$Q_s = [A/B(h)] \cdot q_3(h) \quad (22)$$

$B(d)$ and $B(h)$ were experimentally determined for $g=10$ cm and their behavior is plotted out in Fig. 12, (a) and (b) respectively. From this Fig., it is seen that $B(d)$ increases with a decrease in d , and $B(h)$ increases as h increases.

In addition, $B(d)$ and $B(h)$ could be calculated using the induction coefficient of the probe (D_w), with the assumption that the space charge was distributed along

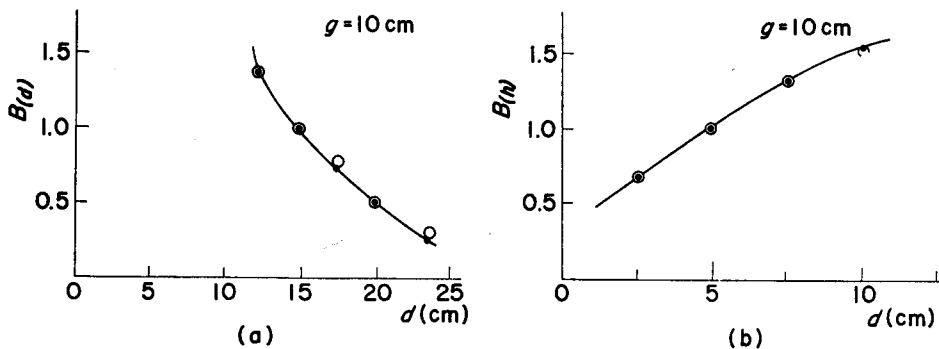


Fig. 12. Variation of $B(d)$ and $B(h)$ with d and h respectively.
 (●----- calculated result, ○----- experimental result)
 (a) $h=5$ cm, $r_{pr}=0.5$ cm
 (b) $d=15$ cm, $r_{pr}=0.5$ cm

the gap axis with the charge density [ρ (C/cm)] constant. In this case, the induced charge on the probe is given by Eq. 23 for the various probe positions.

$$q_3 = \rho \int_0^g D_3 dz \quad \dots\dots (23)$$

Hence, $B(d)$ and $B(h)$ can easily be calculated using Eq. 20. These calculated values are also presented in Fig. 12, and are in good agreement with the experimental values.

3.3 Probe current polarity

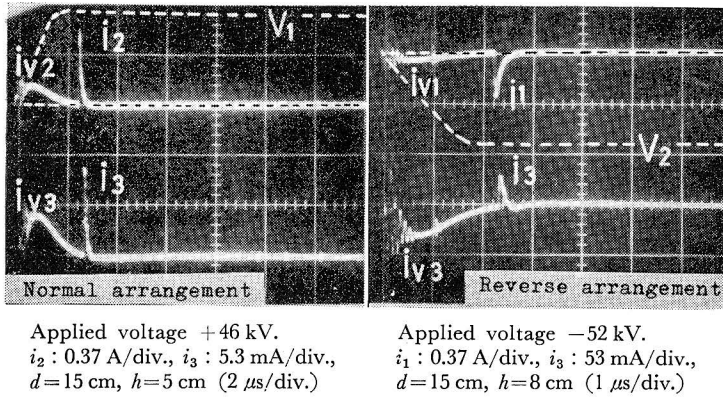
The direction of the current of the rod (i_1) and of the plane (i_2) depend on the polarity of the applied voltage.

Thus, the polarities of i_1 for the reverse arrangement and i_2 for the normal arrangement are coincident with the polarities of the applied voltage. However, the polarity of the probe current (i_3) of the differential circuit depends on the polarity of the space charge, as represented in Eq. 6, provided that the magnitude of the space charge increases following the corona growth.

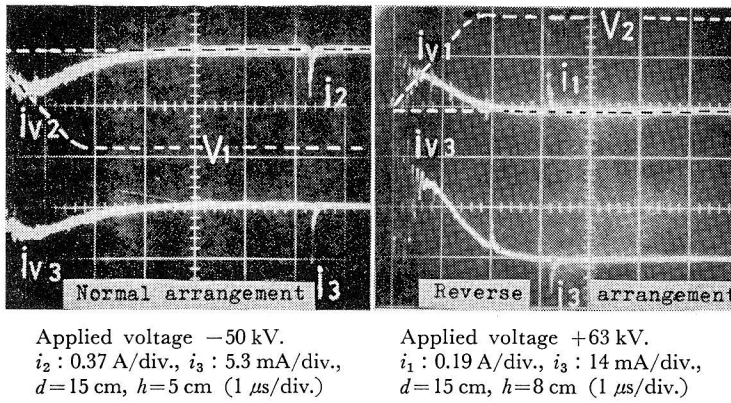
To explain this relationship, the experiment was performed as follows: the polarity of the space charge was changed by a combined change in the gap arrangement and the applied voltage. For example, a positive space charge can be produced either by applying positive voltage to the rod in a normal arrangement, or by applying negative voltage to the plane in reverse arrangement. In these arrangements, the positive corona streamer (PS) propagates from the rod towards the plane, and produces the positive space charge in the gap. In the other arrangements, the negative corona streamer (NS) propagates from the rod towards the plane, and produces the negative space charge in the air gap.

The currents measured in the four cases are shown in Fig. 13. In all cases, the displacement currents ($i_{v1} \sim i_{v3}$) appear first, as shown in Fig. 13. The pulsive currents ($i_1 \sim i_3$) of comparatively short duration are produced by the corona. In each case, the polarities of i_{v1} and i_{v2} coincide with those of the applied voltage, as mentioned earlier. On the other hand, the polarity of i_3 is always positive for PS (See Fig. 13 (a).) and negative for NS. (See Fig. 13 (b).) They are independent of the polarities of the applied voltage. Thus, it is obvious that the polarity of i_3 depends only on the polarity of the space charge. In other words, the polarity of the space charge can be analyzed by observing i_3 .

This method was applied in the analysis of the corona development in the sphere to a rod arrangement. In this case, a negative impulse voltage was applied to the sphere with the rod earthed through a resistance of 10Ω . Fig. 14 shows the oscillographs i_1 and i_3 measured simultaneously, and also shows a still



(a) Currents by PS



(b) Currents by NS

Fig. 13. Oscillographs of probe currents due to PS and NS. ($g=10$ cm)

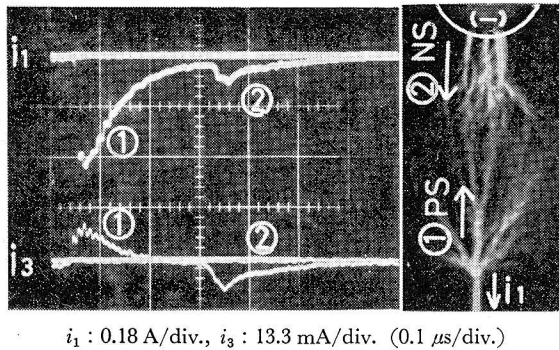


Fig. 14. Oscillographs of i_1 and i_3 for sphere-rod arrangement. (sphere radius; 3 cm, $g=10$ cm, applied voltage; -64 kV)

photograph of the corona. With reference to the still photograph, it is obvious that both electrodes produce coronas. Then, two pulses are produced by the coronas, as indicated by ① and ② on the first and the second pulses respectively. From the oscillograph, since the polarity of i_3 is positive for the first pulse and negative for the second pulse, it is found that PS propagates first from the earthed rod, and produces the positive space charge. Then, NS propagates from the sphere and produces a the negative space charge in the gap.

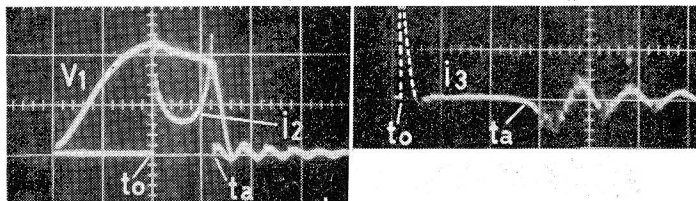
3.4 Discrimination between glow and corona discharges

With reference to Fig. 9, the duration of i_3 for the corona is coincident with that of $i_d(=J)$ which flows through the rod. On the other hand, the induced current in every conductor is considered to be zero for a glow discharge. Hence, the currents i_1 , i_2 and i_3 , which are presented by Eqs. 12, 13 and 6 respectively, are given by

$$i_3 = 0, \quad i_1 = i_2 = J_{con}. \quad \dots\dots(24)$$

This relation is important for discriminating between the corona and glow discharges. Using this knowledge, the development of discharge in a rod-plane gap under low pressure was analyzed as follows.

The experiment was performed in a vacuum chamber at a pressure of 160 Torr. by applying a 50% flashover voltage to the rod. Currents i_2 , i_3 and the voltage across the gap (V_1) were observed, as shown in Fig. 15. With reference to i_2 and V_1 , the discharge starts at time $t=t_0$ and the flashover is maintained at $t=t_a$. During this period V_1 keeps about 40 kV and decreases to nearly zero at $t=t_a$, while i_2 keeps about 40 A. On the other hand, i_3 flows only for a short period of about 0.2 μ s with a peak value of about 160 mA. After this period, i_3 keeps zero till the flashover is maintained. At $t=t_a$, owing to the reduction in the value of V_1 , i_3 turns negative. From these facts, it was found that the discharge started with the corona formation at $t=t_0$, and developed into a glow discharge



V_1 : 20 kV/div., i_2 : 40 A/div. (1 μ s/div.), i_3 : 50 mA/div. (0.5 μ s/div.)

Fig. 15. Oscillographs of V_1 , i_2 and i_3 for glow discharge maintained in a vacuum chamber with 160 Torr., air. ($g=10$ cm, $d=17$ cm, $h=5$ cm)

followed by maintaining the flashover of the gap at $t=t_a$. In addition, the space charge Q_s , generated in the gap during the time $t=t_0 \sim t_a$ was calculated, using Eq. 21, and it was found to be 2×10^{-8} C. This was very small compared to the charge that flowed from the plane to earth ($Q_d^{(1)} = 6 \times 10^{-5}$ C).

4. Conclusion

A method for analyzing the magnitude and the polarity of a space charge by using a small sphere as a probe has been shown theoretically and experimentally. The method has two circuits to measure the space charge. One of them is a differential circuit which detects the induced current flowing through the probe to earth. The other is an integral circuit which detects the induced charge on the probe. The former is suitable for measuring a space charge changing its quantity in ns order accompanied by a growth of the discharge. The latter is suitable for measuring the space charge changing in ms order. The induced charge is proportional to the space charge in the gap and the constant of the proportionality can be given both by experiment and also by calculation. Therefore, the magnitude of a space charge in the gap can be estimated from the induced charge using the constant.

Since the current of the differential circuit flows toward the direction depending on the space charge polarity, it is possible to analyze the polarity of the space charge from the current.

Furthermore, the induced current of the probe is zero after the discharge developed into a glow discharge. This relation makes it possible to discriminate between corona and glow discharges.

The disturbance of the electric field in the gap caused by the introduction of the probe is calculated to be negligible.

From these results, it is confirmed that this method is useful for the measurement of space charge and for the analysis of the process of discharge in the air gap.

Reference

- 1) J. J. Krizinger; Proc. 6th. Int. Conf. Phenomena in Ionized Gases, (1963) p. 295
- 2) M. M. C. Collins & J. M. Meek; Proc. 7th Int. Conf. Phenomena in Ionized Gases, (1965) p. 581
- 3) E. M. Bazelyan; Soviet Phys. Tech. Phys., 9, (1964) 370
- 4) R. T. Waters, T. E. S. Ricard & W. B. Stark; Proc. Roy. Soc. A 304, (1968) 187
- 5) R. T. Waters, T. E. S. Ricard & W. B. Stark; *ibid.*, A 315, (1970) 1
- 6) Oh C. H., Hayashi M. & Uenosono C.; Material of Discharge Seminar, ED-74-15 (1974)
- 7) Isa H., Hayashi M. & Uenosono C.; *ibid.* ED-79-29 (1979)
- 8) Hayashi J. & Kondo B.; Memories of Faculty of Engineering, (1955-3) p. 81
- 9) Shibuya G., etc.; J.I.E.E., 99A, (1979) p. 200

- 10) M. A. Harrison & Geballe; Phys. Rev., 91 (1953) 1
- 11) W. Shockley; J. Appl. Phys., 9, (1938) 635
- 12) Y. Murooka, T. Hirano & K. Kishi; J. Appl. Phys., 46 (1975) 2005